Cent. Eur. J. Chem. • 10(1) • 2012 • 105-112
DOI: 10.2478/s11532-011-0123-6

VERSITA

Central European Journal of **Chemistry**

Synthesis of aluminosilicates under high pressure and using sulfur as directing agent

Research Article

Sandra Loera[1*], Enrique Lima[2], Heriberto Pfeiffer[2], Victor H. Lara[3]

[1]*Metropolitan Autonomous University-Azcapotzalco, Col. Reynosa Tamaulipas Azcapotzalco, 02200, México D.F. Mexico*

[2]*Materials research Institute, National Autonomous University of Mexico, Circuito exterior s/n, Cd. Universitaria CP 04510, México. D. F. Mexico*

[3]*Metropolitan Autonomous University- Iztapalapa, Col. Vicentina, 09340, México D. F. Mexico*

Received 20 May 2011; Accepted 14 September 2011

Abstract: Two aluminosilicates were prepared under hydrothermal conditions. Silica, sodium aluminate, sodium sulfide and sulfur were used as raw materials. Starting with similar reacting mixtures, analcime (zeolite, $Na(Si_2Al)O_6 \cdot H_2O$) and beidellite (clay, $Na_{0.3}Al_2(Si, Al)_4O_{10}(OH)_2 \cdot 2H_2O$) were synthesized by varying pressures, 2 kbar and 1 kbar, respectively. Sulfur was present in both aluminosilicate surfaces, which confer to them particular adsorption properties. Additionally, water adsorption isotherms, under dynamical conditions, were obtained. Fractal dimension values and SEM micrographs reveal very different textural and morphological properties of the two prepared aluminosilicates.

Keywords: *Beidellite • Catalysts • Sulfur • Analcime • Small-angle X-ray scattering*

1. Introduction

Zeolites occur naturally, they are formed where volcanic rocks and ash layers react with alkaline groundwater. Generally, the crystallization of minerals in volcanic rocks occur through interactions between fluids with pre-existing crystal phases and with glass, the latter representing the most abundant fraction in pyroclastic materials [1]. The chemical composition of the glass plays a crucial role in the resulting mineral and the kinetics reaction. Actually, silica-rich glasses are not very reactive. Temperature, fluid composition, and pH are also important factors driving reaction kinetics [2]. Thus, geological conditions are determinant to crystallized sediments as chabazite, analcime and phillipsite, amongst other zeolites. Even though zeolites occur naturally, the synthetic ones are the most widely used as sorbents, catalysts, support catalysts and ion-exchange materials. The most common synthetic way to prepare zeolites is *via* hydrothermal treatment at moderate temperatures (~200 ºC) and elevated pressures in presence of excess water [3].

Physicochemical parameters are, of course, determinant for synthesis. Largely, temperature and pressure effects have been studied on hydrothermal synthesis of zeolites [4-6]. It is possible to drive the synthesis to obtain different aluminosilicates starting from same reactants, for example, as in the four component system of Na_2O-Al_2O_3-SiO_2-H_2O at 1013 bars, and excess of water. Synthetic phase of albite, analcime, mordenite, hydroxycancrinite, natrolite, nepheline hydrate, hydroxysodalite, and montmorillonite are formed by varying the temperature conditions between 290 and 700ºC [7,8].

Before the growth of crystalline aluminosilicates such as zeolites, a nucleation step is required. Therefore, during synthesis, inorganic or organic molecules are used to direct the crystallization towards a specific zeolitic structure. Water molecules act as void fillers,

* *E-mail: sls@correo.azc.uam.mx*

stabilizing the porous framework. Interactions of water molecules with cations are of crucial importance to direct the structure [9,10]. In this context, sulfur is an exciting element which can be used as director agent. Sulfur, indeed, is commonly found in volcanic rocks and probably is involved in natural zeolite genesis. Incorporation of sulfur in a synthetic route is therefore the motivation. The synthesis of analcime under high pressure, in the absence of sulfur is well documented [3]. Zeolite type, porosity and cavity sizes could therefore be tuned by the size of the sulfur chains.

Zeolites have a great capacity to host many chemical species, mainly water and cations. The structure determines the zeolite capacity as adsorbents and their selectivity of shape. In this context, Line and coworkers [4] have studied the dehydration kinetics on two analcime structures. The first one was X-analcime that is formed by ion exchange fromLeucite and has a surface area of 20 m^2 g^{-1} while the second one was H-analcime that is synthesized by hydrothermal conditions and has 2 m^2 g^{-1} of surface area. The porous network, which is determined by parameters of synthesis, is responsible for the adsorption capacity.

In this work, we present the effect of pressure and time on aluminosilicate synthesis by hydrothermal conditions using sulfur as directing agent at 280ºC. The aluminosilicates were prepared using silica, sodium aluminate, sulfur and sodium sulfide as precursors. We also determined hydration and dehydration behavior of samples synthesized.

2. Experimental procedure

2.1. Materials

All reagents employed were commercially available and used as supplied without further purification. Sodium aluminate was obtained from Fisher Scientific, while hydrophilic fumed silica Aerosil 130, from Degussa, was used as silicon reagent. Sulfur (99.999%, golden label) and sodium sulfide (≥ 98.0%) were obtained from Aldrich.

2.2. Synthesis

Sodium aluminate, silica and sulfur and sodium sulfides were ground together in a molar ratio of 1.0:1.0:0.94:0.23, respectively. Teflon containers having a capacity of 16 cm^3 were filled with 12.8 cm^3 of the mixture, then 3.2 mL of water was added, the containers sealed and placed in an autoclave. Teflon was used because it did not alter significantly under high pressure hydrothermal conditions up to 280ºC, even for 60 day duration of synthesis period [10]. All hydrothermal experiments were performed using high pressure autoclaves (type AE 0010AS22 1517, Autoclave Engineers, USA) with Bridgeman sealing technique at a static water pressure. The furnaces were placed vertically in order to maintain a constant temperature gradient. Once both furnace and autoclave reached the thermal equilibrium, the external water pressure was applied using a piston pump (Sitec, Switzerland) with distilled water as the pressure medium until a stable final static hydraulic pressure was attained. Once the synthesis time was accomplished, the heating of the furnace was stopped when a simultaneous drop in temperature and pressure occurred.The temperature maintained during synthesis was 280ºC.

Two different samples were synthesized, $SiAl_Z$ and $SiAl_C$. The $SiAl_Z$ sample was synthesized at 2 kbar of pressure and required a reaction time of 23 days. The $SiAl_C$ sample was obtained at 1 kbar of pressure after a reaction time of 46 days. All samples were filtered and washed several times with deionized water to eliminate soluble residues, dried and characterized.

2.3. Characterization

Materials were characterized by energy dispersive X-ray spectroscopy (EDX) , X-ray diffraction (XRD), scanning electron microscopy (SEM), small-angle X-ray scattering (SAXS), ^{29}Si and ^{27}Al solid state nuclear magnetic resonance spectroscopy (NMR), and different thermogravimetric analyses.

The energy dispersive X-ray spectroscopy was performed with an EDS, EDAX DX4 SUTW-USA, coupled to a Cambridge S90B scanning electron microscope, Great Britain system. Focus of beam assures covering an area of 6 μm^2 and a depth of 4 µm. A powder diffractometer (Siemens D500) coupled to a copper anode X-ray tube was used to identify compounds present in each sample. The Kα1 radiation was selected with a diffracted beam monochromator. Scanning electron microscopy (SEM with field emission cathode, Philips XLS 30 ESEM) gave morphological information such as particle size and shape, dispersion of the powders and other microstructural properties of the samples.

A Kratky camera coupled to a copper anode X-ray tube was used to measure the SAXS curves. The sample was introduced into a capillary tube. The distance between the sample and the linear proportional counter was 25 cm; a Ni filter was selected for the Cu Kα radiation. Intensity I(h) was measured for 9 min in order to obtain good quality statistics. The data was collected with a proportional linear counter and analyzed as reported by Glatter's ITP92 program [11-13]. From the slope of the plot of the logarithm of the corrected intensity, log I(h), versus the logarithm of the angular parameter,

log h; where h = 2π sin θ/λ with θ defined as the scattering angle and λ as the wavelength, the fractal dimension (D_f) was obtained [14]. The shape of the scattering objects was estimated from the Kratky plot, *i.e.*, $h^2I(h)$ *versus* h. Kratky curve profile gives information about shape of scattered objects. For instance, if the curve presents a peak, the particles are globular [15,16]. If a shape can be assumed [13], the size distribution function may be calculated.

The NMR spectra were acquired under magic angle spinning (MAS) conditions on a Bruker Avance II spectrometer with a magnetic field of 7.05 Teslas. The ^{27}Al MAS NMR spectra were recorded at the spectrometer frequency of 78.21 MHz. Short single pulses (π/12) were used; spinning rate was 10 kHz and the chemical shift reference was aqueous $[Al(H_2O)_6]^{3+}$. ^{29}Si MAS NMR spectra were obtained using a resonance frequency of 59.59 MHz with a recycling time of 30 s and a pulse time of 3 μs. The spinning frequency was 5 kHz, and tetramethylsilane (TMS) was used as a reference.

High resolution thermogravimetric analyses (TGA Q500HR, TA Instruments) were used to determine the thermal stability of the samples. Each dynamic thermogram was carried out at 5°C min^{-1} an air atmosphere. Additionally, a Q5000SA thermobalance equipped with a humidity-controlled chamber, from TA Instruments, was used to perform a water sorption analysis.All experiments were performed using N_2 (Praxair, grade 4.8) as carrier gas and distilled water as the vapor precursor using a total gas flow of 100 mL min^{-1}. The relative humidity percentages were controlled automatically with the Q5000SA equipment. Samples were tested as produced (native) and thermally activated at 600ºC for 4 hours.

3. Results and discussion

X-Ray diffraction patterns of $SiAl_Z$ and $SiAl_C$ samples are compared in Fig. 1. At the XRD detection limit, both XRD patterns showed the formation of pure but different phases. While, the $SiAl_Z$ diffraction pattern correlated with the analcime structure (a zeolite, $Na(Si_2Al)O_6 \cdot H_2O$, with JCPDS 19-1180), the $SiAl_C$ sample matched with the beidellite, a clay ($Na_{0.3}Al_2(Si, Al)_4O_{10}(OH)_2 \cdot 2H_2O$, with JCPDS 43-0688). Peaks labeled as Pt correspond to (111), (200) and (220) planes of the platinum sample holder. The $SiAl_Z$ XRD pattern corresponds to fully crystalline analcime, which is an orthorhombic crystalline system. Position of peaks (400), (604) and (611) was precisely measured using the peak (111) of Pt as external reference. The cell parameters were calculated to be 13.67, 14.26 and 13.67 Å (± 0. 06 Å).

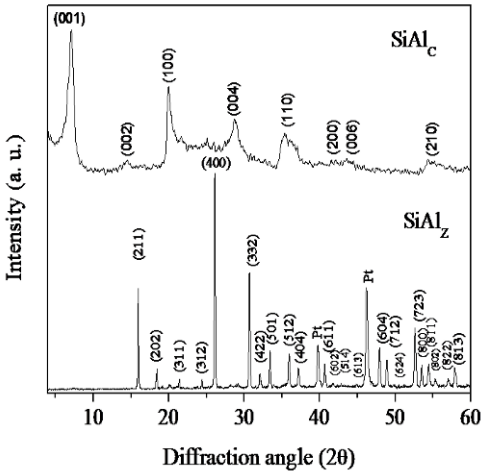

Figure 1. X-ray diffraction patterns of $SiAl_Z$ and $SiAl_C$. Each diffraction pattern was indexed with the corresponding JCPDS card; 19-1180 for $SiAl_Z$ and 43-0688 for $SiAl_C$. Peaks labeled as Pt correspond to platinum support (4-0802 JCPDS card).

Conversely, the XRD pattern of $SiAl_C$ sample fitted with a beidellite laminar structure, with a hexagonal crystalline cell: a_0 = 5.11 Å and c_0 = 12.55 Å. The material was characterized as d(001)-spacing equal to 12.55 Å which is close to the literature reported value of 12.6 Å, [7]. Thus, pressure induces the formation of different structures; a higher pressure produced a denser material (zeolite), as it could be expected. Additionally, the crystal size, of both samples, was obtained from profile fitting of the 100% intensity diffraction peak according to the Scherrer equation, being 102.9 Å and 614.9 Å for $SiAl_C$ and $SiAl_Z$, respectively. The crystal size has larger rising synthesis pressure this result being consistent with pressure. Some papers suggest a hydrothermal synthesis mechanism, which consists of precursor dissolution, supersaturation of the hydrothermal fluid and the consequent recrystalization from the supersaturated solution [8,17].

The chemical composition of $SiAl_Z$ and $SiAl_C$ as determined by EDX is shown in Table 1. The ideal composition determined by the structural formula reported in JCPDS cards, was also included. The Si/Al molar ratio 2.07 for analcime and beidellite was different from the Si/Al=1.32 and 1.93 ratios that were obtained for the,$SiAl_Z$ and $SiAl_C$ respectively. Such a difference cannot be explained simply as the zeolite and clay compounds as identified in XRD. This result is related to the resolution and main principles of EDX technique, indeed EDX is a surface analysis corresponding to an area of 6 μm^2 and a depth of 4 μm [18]. Nevertheless, the elemental compositions of the synthesized samples are in the range of analcime and beidellite and the XRD pattern was readily indexed as orthorhombic analcime

Table 1. Chemical analysis of aluminosilicates as determined by EDX, and the theoretical values of analcime and beidellite.

Element	Composition (wt%)			
			Ideal	
	$SiAl_Z$	$SiAl_C$	Analcime	Beidellite
O	48.23	42.06	50.90	47.65
Na	9.07	3.01	10.45	1.70
Al	16.27	16.16	12.27	13.40
Si	21.45	31.24	25.45	27.80
S	4.99	7.53	0	0

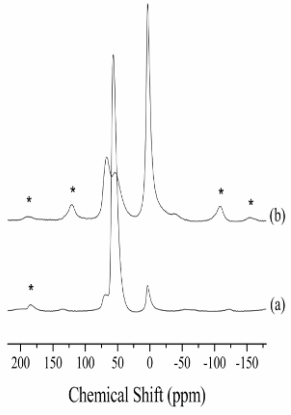

Figure 2. ^{27}Al MAS NMR spectra of samples (a) $SiAl_Z$ and (b) $SiAl_C$. * indicates spinning side bands (10 kHz).

($SiAl_Z$) and hexagonal beidellite ($SiAl_C$). Note that sulfur found, on the surface of $SiAl_C$ was higher than that observed on the $SiAl_Z$ sample. This difference does not correspond to the expected sulfur composition of the surfaces, because the same amount of sulfur was used during material synthesis. The difference in sulfur (2.54 wt%) may be attributed to occlusion of sulfide species into the aluminosilicate network. It seems that more sulfur reached the bulk of the clay, in comparison to the zeolite. It must be noticed that sodium content was rather low compared to other similar materials.

Fig. 2 displays the ^{27}Al NMR spectra of both samples. Typical ^{27}Al NMR spectra of free-sulfur analcime present a single peak near to 50 ppm [19]. On the contrary, $SiAl_Z$ spectrum is composed by three isotropic peaks located at 3.7, 55 and 72 ppm. First two peaks can be attributed to six-fold and four-fold coordinated aluminum in an oxygen environment, respectively. Third peak, at 72 ppm, is shifted toward lower field and cannot be assigned to tetrahedral AlO_4. However, the NMR signals of AlS_4 species are expected to appear close to 90-100 ppm. Then, it is possible that the peak located at 72 ppm in the analcime spectrum is due to aluminum bonded to oxygen and sulfur atoms, *i.e.*, this result seems to confirm the hypothesis that some sulfide species were stabilized in a way that $AlO_{4-x}S_x$ species, with values possible for x of 1, 2 or 3. $SiAl_C$ NMR spectrum present the same three peaks observed in the spectrum of $SiAl_Z$, but with very different relative intensities. The signal at 3.7 ppm for the octahedral aluminum species are dominant in the clay spectrum. However, a large amount of tetrahedral aluminum close to oxygen and sulfur is also detected as shown by peaks located at 72 ppm. The intensities agree with the proportion of tetrahedral to octahedrally coordinated aluminum expected for beidellite clay; clay built up from two tetrahedral and one octahedral sheets. It can be seen that there is more tetrahedral Al (signal at 55 ppm) in the $SiAl_Z$ sample than in the $SiAl_C$ sample. It should be mentioned that from the differences observed in the ^{27}Al NMR peak widths, it is difficult to make a fine quantitative assessment of the proportion of aluminum species.

Furthermore, ^{29}Si NMR spectra (Fig. 3) reveal seven signals at -109, -104, -99.1, -93.8, -88.5, -84 and -81 ppm for the $SiAl_Z$ sample. The first five signals are roughly shifted to 5 ppm low field for each of aluminum's next-nearest- neighbor, therefore they are assigned to Si tetrahedrally coordinated with 4 Al, 3 Al and 1 Si, 2Al and 2 Si, 1 Al and 3 Si, and 4 Si second nearest neighbors, respectively [20-22]. These signals are hereafter referred as Si(nAl), where n is the number of Al atoms in the second nearest neighbor coordination shell. It should be noticed that the presence of 5 signals for analcime zeolite is unusual. The analcime structure was described to be built by silicon-containing four-rings which are connected through aluminum atoms. Thus, it would be expected that only Si(2Al) groups were present in a well analcime ordered lattice. Actually, the Si(nAl) signal, in the range of Si(2Al) units, shows the highest intensity, but it is accompanied by other signals of relatively high intensity, supporting thus a not fully ordered lattice. On the other hand, since ^{29}Si MAS NMR shifts for aluminosilicates are typically in the range from - 87 to - 110 ppm [19], two signals, at -84 and -81 ppm cannot be assigned to SiO_4(nAl) units in analcime structure. Therefore, ^{29}Si NMR results confirm a new environment for Si and Al nuclei induced by the presence of sulfur.

Concerning beidellite, which is a dioctahedral member of the smectite group, the ^{29}Si NMR spectrum exhibit well defined peaks at about -94, -86 and -82 ppm corresponding to Si bonded to (0AlIV, 2AlVI), (1AlIV, 2AlVI), and (2AlIV, 2AlVI), respectively [23]. There was not observed the presence of additional signals, supporting the idea that silicon is fully incorporated to clay. With this clay assignment, it seems that in analcime sample, some clay particles could be present.

A SEM image of the $SiAl_Z$ sample is presented in Fig. 4, where polyhedral particles as large as 150 μm are observed. At higher magnifications, it can be seen

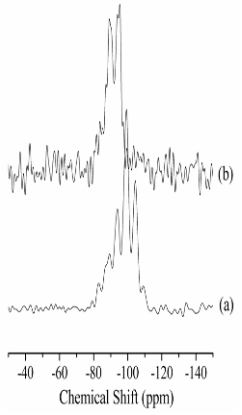

Figure 3. ^{29}Si MAS NMR spectra of samples (a) $SiAl_Z$ and (b) $SiAl_C$.

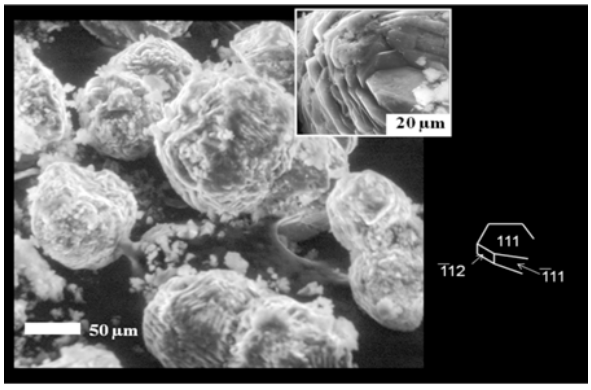

Figure 4. SEM image of $SiAl_Z$ sample. Grains of around 150 μm of size are observed, which are mostly agglomerates of smaller particles (15 μm). These particles presented a layered morphology.

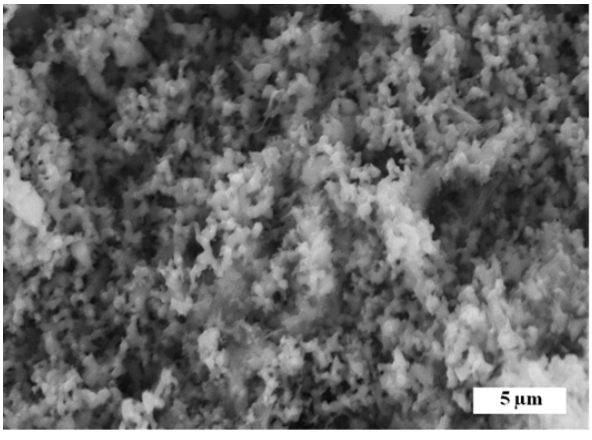

Figure 5. SEM micrograph of beidellite particles of about 1 μm of diameter obtained after 46 days at 280ºC (1 kbar of pressure).

that polycrystalline particles are the consequence of self-assembled oriented platelets in the [111] plane [5]. Single grains, smaller than 15 µm, were formed and then the second particles generation as layer (c.a. 10 µm) formed on the primary single grain indicates that the supersaturation limit was reached at least a second time during the synthesis process, leading to a oriented growth. Fig. 5 presents SEM images of sample $SiAl_C$. SEM picture showed an irregular morphology of particles smaller than 1µm which agglomerate. The morphology of this sample differs significantly if compared with $SiAl_Z$ sample. These differences can be attributed to combined action of the pressure and synthesis time.

Fig. 6 compares the Kratky plots of samples $SiAl_Z$ and $SiAl_C$. The intensity of scattering profiles of both samples, $SiAl_C$ and $SiAl_Z$, are proportional to scattering vector as a function of h^{-4} which has large h values and h^{-2} for moderate h values. Hence, the Kratky plot exhibits a clear peak, which is the case of scattered heterogeneities that have a globular or spheroid shape. Fractal dimension values, as determined from SAXS data, differ for both samples. The fractal dimension of 2.2 for sample $SiAl_C$ indicates that clay exhibit a relatively low roughed surface. On the contrary, $SiAl_Z$ sample exhibit a fractal dimension of 2.8 which is a value consistent with spheroid particles which are not completely smoothed but they contain free spaces and edges because of the not fully ordered assembly of platelets, in agreement with observed by SEM.

Fig. 7 shows the $SiAl_Z$ and $SiAl_C$ thermograms. As expected, according to the structural and morphological characterizations, the samples presented different thermal behaviors. $SiAl_Z$ sample, which possesses an analcime zeolitic structure, did not lose weight between room temperature and 160°C. Then, between 160 and 390°C, this sample lost 7.1 wt%, attributed to water evaporation of molecules located in the zeolitic channels. Finally, between 445 and 552°C the sample lost 0.4 wt%. In this temperature range it is not expected to lose weight in pure analcime therefore, the loss may then be attributed to decomposition of sulfur species. On the other hand, as expected, the $SiAl_C$ sample presented a different thermal behavior. Initially, from room temperature to 360°C the sample lost weight exponentially (4.3 wt%) that can be attributed to the water evaporation of superficial and interlayered molecules. After the dehydration process, the sample presented a second weight loss equal to 2.7 wt% (370-540°C), which corresponded to the dehydroxylation process, and consequently, to the layered structure destruction. Finally, the sample lost 0.8 wt%, between 560 and 650 °C, which may be attributed to loss of sulfur as in case of analcime sample. Note that the amount of sulfur lost in zeolite and clay agrees, with the relative amount of sulfur detected by EDX analysis at the particle surfaces.

For thermally stability results, a portion of the samples was heat treated at 650°C for 6 hours, in order

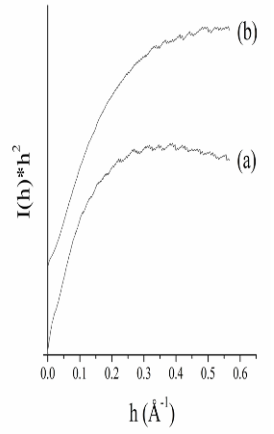

Figure 6. Kratky profiles of the samples (a) $SiAl_Z$ and (b) $SiAl_C$ samples.

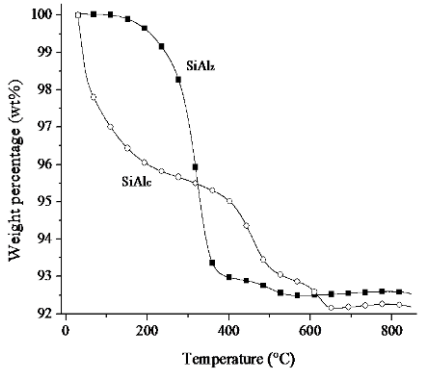

Figure 7. Dynamic thermograms of the $SiAl_Z$ and $SiAl_C$ samples.

to eliminate all the water, hydroxyl and other species of the samples prior to analysis of the water sorption phenomena. Fig. 8 shows different water adsorption-desorption isotherms of the $SiAl_Z$ sample, original and thermally treated at 650°C. As it can be seen during the adsorption process, all the curves presented isotherms of type III which, according to the IUPAC, correspond to weak attractive adsorbate-adsorbent interactions, and the adsorbate-adsorbate interactions plays an important role [24]. After that, desorption or dehydration process varied as a function of the thermal treatment. $SiAl_Z$ sample previously treated at 650°C Initially adsorbed more water as a function of temperature. Water adsorbed increased from 0.91, 1.05 and 1.11 wt% if the adsorption process was produced at 50, 60 or 70°C, respectively. Of course, the quantities of water adsorbed are very low, in comparison to the water desorption produced during the thermal activation (see Fig. 7). Additionally, in these cases the desorption processes was not completed, as 0.2-0.3 wt% of the total adsorbed water remained at the end of the desorption process. Therefore, these water molecules must have been adsorbed over the zeolite surface and only a very small quantity of water diffused

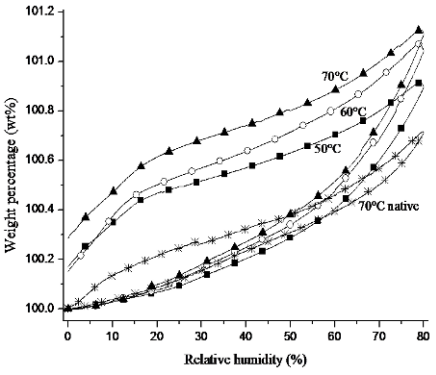

Figure 8. Water adsorption-desorption isotherms of the $SiAl_Z$ native sample and after a thermal treatment at 650°C. The isotherms were performed at 70 (native and thermally treated samples) and 60 and 50°C (sample thermally treated).

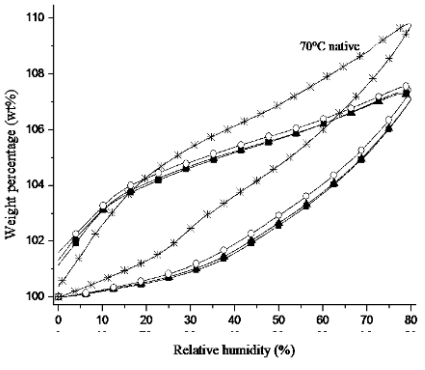

Figure 9. Water adsorption-desorption isotherms of the $SiAl_C$ native sample and after a thermal treatment at 650°C. The isotherms were performed at 70 (native and thermally treated samples) and 60 and 50°C (sample thermally treated).

into the zeolitic channels, inhibiting their desorption at the thermal conditions. However, the $SiAl_Z$ original sample, which was only tested at 70°C, was the sample that adsorbed less water (0.71 wt%), and in this case all the water was desorbed. Hence, the previous thermal treatment cleaned surface and the zeolitic channels. However, it has to be mentioned that water adsorption was, in fact, low and most of it was only superficially adsorbed.

Although $SiAl_C$ presented the same kind of isothermal behavior as $SiAl_Z$, the water adsorbed was much higher in this case (Fig. 9). Samples thermally treated at 650°C adsorbed up to 8 wt% and the residual water was 1% in all the cases. Nevertheless, in this case, the original sample was the sample which adsorbed more water 10.2 wt%, but this sample practically desorbed all water at the end of the desorption process. In this case, thermal activation did not improve water adsorption, although in all the cases it was always higher than that obtained in the zeolite structure. It may be explained in

terms of external surface area, which must be higher in the $SiAl_C$ sample.

Contrary to conventional materials synthesis, in this work sulfur was used as a directing agent during the hydrothermal synthesis. When the synthesis pressure was 1 kbar the resulting material was a clay ($SiAl_C$, beidellite). Upon increase in pressure to 2 kbar the resulting material was a zeolite ($SiAl_Z$, analcime). Clearly, the pressure was a key parameter to drive the synthesis of aluminosilicate is directly related to changes observed on sulfur with pressure.

Actually, the analysis of low-pressure phase diagram of sulfur [25] under isobaric conditions (1 kbar), illustrate that at room temperature sulfur possesses an orthorhombic crystal structure. At around 170-190ºC the sulfur liquid phase appears and 190ºC was precisely the temperature maintained for synthesis of the aluminosilicates. The sulfur prevailing molecular species, during the synthesis of $SiAl_C$ sample, are cyclo-octa sulfur however, a high amount of Sn chains, catena or mixed cyclo linear species are expected to be present. Thus, during the standard hydrothermal synthesis under isobaric conditions without agitation, the experiment begins with water as fluid with solid precursor materials. With time, the mixture gets more concentrated , until a supersaturated state is produced. At a certain level of supersaturation a spontaneous crystallization occurs, leading to a decrease of in the concentration of the hydrothermal fluid [17]. The high amount of sulfur in this sample, as determined by EDX analysis, can be explained because of the presence of highly disrupted cyclo-octa sulfur which is easily incorporated into the clay structure being either adsorbed at surface of the clay or as interlayered stable species. Nevertheless, the distribution of sulfur species is not fully homogeneous and electronic density is heterogeneously distributed leading to heterogeneously sized small particles that form agglomerates with a low density as revealed by the fractal dimension, as determined by SAXS.

If pressure is increased up to 2 kbar, sulfur is at the frontier where solid orthorhombic remains, *i.e.*, S_8 species are the main molecules present. Actually, under this pressures the S_8 adopts a crown configuration [26]. It could be possible that at 2 kbar and 190°C S_8 rings collapse to give liquid sulfur therefore, the material crystallizes mainly as analcime and formation of big agglomerates is favored because of ordered sulfur species that drives stacking of small particles. During this crystal grown, under high pressure and for long times, the formation of O-Al-S bonds seem to be possible as suggested the ^{27}Al NMR results. At end of crystal growth step, big globular particles with rough surfaces are obtained which, interestingly, presents strong water adsorption sites, an can be explained as polarized O-Al-S groups immersed into the zeolite matrix. In contrast, the clay structure allows the deposition of water interlayers more easily than the zeolite. Nevertheless, thermal activation decreased the water adsorption capacity, perhaps as part of superficial sulphur was lost.

4. Conclusions

Hydrothermal synthesis of aluminosilicates can be tuned to obtain either beidellite clay or analcime zeolite. By using sulfur as a directing agent, a functionalization with sulfur centers on the surface of both the aluminosilicates is induced. These sulfur centers, together with aluminum cations, can play the role of strong adsorption sites to adsorb polar molecules such water. Morphology of clay and zeolites were clearly different. On one hand nearly globular particles of analcime were built by a stacking of smaller particles well oriented on the 111 plane and on the other hand small clay particles were formed with an irregular shape. Clay and zeolite differed also in their fractal dimensions. Polyhedral particles of analcime presented a roughened surface because of the defects such as edges of stacked smaller particleswhile the particles of clay agglomerate gave smooth surfaces.

Acknowledgment

The authors would like to thank the financial support through the CONACyT project 154736.

References

[1] D.W. Breck, Zeolites Molecular Sieves. Structure, chemistry, and use (A Wiley-Interscience Publication, New York, 1974) pp. 245
[2] C.S. Cundy, P.A. Cox, Chemical Reviews 103, 663 (2003)
[3] H. Ghobarkar, O. Schäf, Y. Massini, P. Knauth, The reconstruction of natural zeolites (Kluwen Academic Publishers, Netherlands, 2003) pp. 22
[4] C.M.B. Line, A. Putnis, C. Putnis, C. Giampaolo, American Mineralogist 80, 268 (1995)
[5] H. Ghobarkar, O. Schäf, Materials Science and Engineering B60, 163 (1999)
[6] H. Ghobarkar, O. Schäf, B. Paz, P. Knauth, Journal of Solid State Chemistry 173, 27 (2003)
[7] L. Belaroui, J.M.M. Millet, A. Benguedach, Catalysis Today 89, 279 (2009)

[8] O. Schäf, H. Ghobarkar, A. Garnier, C. Vagner, J.K.N. Lindner, J. Hanss, A. Reller, Solid State Sciences 8, 625 (2006)
[9] A. Corma, F. Rey, J. Rius, M.J. Sabater, S. Valencia, Nature 431, 287 (2004)
[10] H. Ghobarkar, O. Schäf, U. Guth, Progress in Solid State Chemistry 27, 29 (1999)
[11] O. Glatter, Journal of Applied Crystallography 14, 101 (1981)
[12] O. Glatter, B. Hinisch, Journal of Applied Crystallography 17, 435 (1984)
[13] O. Glatter, Progress in Colloid and Polymer Science 84, 46 (1981)
[14] A. Guinier, G. Fournet, Small-Angle Scattering of X-rays (John Wiley & Sons: New York, 1955) 37
[15] M. Kataoka, Y. Hagihara, K. Mihara, Y. Goto, J. Mol. Biol. 229, 591 (1993)
[16] M. Kataoka, J.M. Flanagan, F. Tokunaga, D.M. Engelman, In: B. Chanse, J. Deisenhofer, S. Ebashi, D.T. Goodhead, H.E. Huxley (Eds.), Use of X-ray Solution Scattering for Protein Folding Study in Synchrotron Radiation in the Biosciences (Clarendon Oxford Press, London, 1994) pp. 4, 87
[17] O. Schäf, H. Ghobarkar, P. Knauth, In: P. Knauth, J. Schoonman (Eds.), Hydrothermal synthesis of nanomaterials Nanostrructurates Materials: Selected Synthesis Method, Properties and Applications (Kluwer, Boston, 2002) 8, 23
[18] S. Loera, P.L. Llewellyn, E. Lima, The Journal of Phisical Chemistry C 114, 7880 (2010)
[19] B. Herreros, J. Klinowski, The Journal of Phisical Chemistry 99, 1025 (1995)
[20] E. Lippmaa, M. Magi, A. Samoson, M. Tarmak, G. Engelhard, J. Am. Chem. Soc. 103, 4992 (1981)
[21] B.L. Phillips, R.J. Kirkpatrick, American Mineralogist 79, 1025 (1994)
[22] P. Neuhoff, L. Hovis, L. Balassone, J. Tebbins, American Journal of Science 304, 21 (2004)
[23] N.C. Alma, G.R. Hays, A.V. Samoson, E.T. Lippmaa, Anal Chem. 56, 729 (1984)
[24] S. Lowell, J.E. Shields, M.A. Thomas, M. Thommes, Characterization of porous solids and powders: Surface area, pore size and density (Kluwer Academic publishers, Dordrecht, Netherlands, 2004) 11-14
[25] A.G.M. Ferreira, L.Q. Ferreira, J. Chem. Thermodynamics (In press) doi: 10.1016/j.jct.2010.07.007 (2010)
[26] F.A. Cotton, G. Wilkinson, Advanced Inorganic Chemistry (A Wiley-Interscience Publication, New York, 1999) 502